Aerosol Science and Technology, 46:843–851, 2012
Copyright © American Association for Aerosol Research
ISSN: 0278-6826 print / 1521-7388 online
DOI: 10.1080/02786826.2012.671559

An Exact Solution of Interception Efficiency Over an Elliptical Fiber Collector

Wenxi Wang,[1] Mingliang Xie,[1,2] and Lianping Wang[2]
[1]*The State Key Laboratory of Coal Combustion, Huazhong University of Science and Technology, Wuhan, People's Republic of China*
[2]*Department of Mechanical Engineering, University of Delaware, Newark, Delaware, USA*

Downloaded by [University of Delaware] at 19:53 16 June 2012

An exact solution for the interception efficiency of a particle carried by potential flow over an elliptical fiber acting as the collector has been developed based on the Zhukovsky conversion. It is shown that the interception efficiency depends on fiber geometric properties such as size, aspect ratio, the orientation angle of the incoming flow, and the particle diameter. The results show that the noncircular collector shape can improve the interception efficiency significantly when compared to a circular collector, and the maximum efficiency occurs when the incoming flow is parallel to the major axis of the elliptical fiber.

INTRODUCTION

In recent years, particles deposition phenomenon has received much attention in the energy, environment and chemical industry fields, due to its importance in many applications such as the fouling of the heat exchanger surface of the boiler, the deposition of small particles on micro-electromechanical systems, light transmission components and respiratory, the respirable particles emission from combustion sources. In order to promote the small particle's deposition and capture many researchers have already carried out a lot of studies on the filtering operation. The fabric filter has been widely used due to its simple, convenient, and general features (Parker 1977). To improve the efficiency of a fabric filter, the filtering mechanisms and efficiency become the focus of current research in the field. The single fiber theory is the basis of the classic filtration theory (Hinds 1999; Lee and Mukund 2001), in which the filtration efficiency is mainly determined by 3 mechanisms: (1) impaction; (2) direct interception; (3) diffusion. The total collection efficiency is defined as a superposition of these collection mechanisms. Generally, the classic theory assumes that once a particle touches the fiber, it is captured without bouncing, and that the particles are spherical. Generally, the single fiber efficiency η_F is the sum of the efficiencies from all the 3 individual mechanisms (Kirsch and Fuchs 1967),

$$\eta_F = \eta_R + \eta_I + \eta_D \tag{1}$$

in which η_R is the single fiber efficiency by direct interception, η_I is the single fiber efficiency by impaction, and η_D is the single fiber efficiency by diffusion, as indicated in Figure 1. Interception and inertial impaction play negligible roles in capturing very small particles. On the other hand, for particles larger than 500 nm at normal temperatures and pressures, Brownian diffusion is practically nonexistent, and the collection efficiency is due solely to interception and inertial impaction.

The transport of small particles to the surfaces of filters is virtually a particle-laden 2-phase flow. The flow field influences the deposition of small particles largely, which is proved by some researchers that the more turbulent of the flow field the lesser particles deposit on surface (Song et al. 1996). The particle deposition on the surfaces of filter is considered to involve at least 2 separate and distinct steps: First, the transport of small particles to the surfaces of filters, which is driven by the velocity field around the fiber; second, the attachment of particles to this surface due to near-field physicochemical forces. The first step involves the flow regimes over the obstacles, which include the viscous Stokes flow ($Re < 1$), transition ($1 \leq Re \leq 1000$), and potential flow ($Re \geq 1000$) regimes. For viscous Stokes flow around a circle, Kuwabara (1959) arrived at an analytical description of the flow field by neglecting inertial terms in the Navier–Stokes equations and specifying boundary conditions on a unit cell around each fiber. Happel (1959) also obtained a similar result independently. Since then, the Kuwabara or Happel flow field has been accepted as fundamental to many

Received 27 November 2011; accepted 22 February 2012.
This work is supported by the National Natural Science Foundation of China with Grant No. 50806023 and the National Natural Science Foundation of China with Grant No. 50721005 and the Programmer of Introducing Talents of Discipline to Universities ("111" project No. B06019), China.
Address correspondence to Mingliang Xie, The State Key Laboratory of Coal Combustion, Huazhong University of Science and Technology, 1037 Luoyu Road, Wuhan 430074, People's Republic of China. E-mail: mlxie@mail.hust.edu.cn

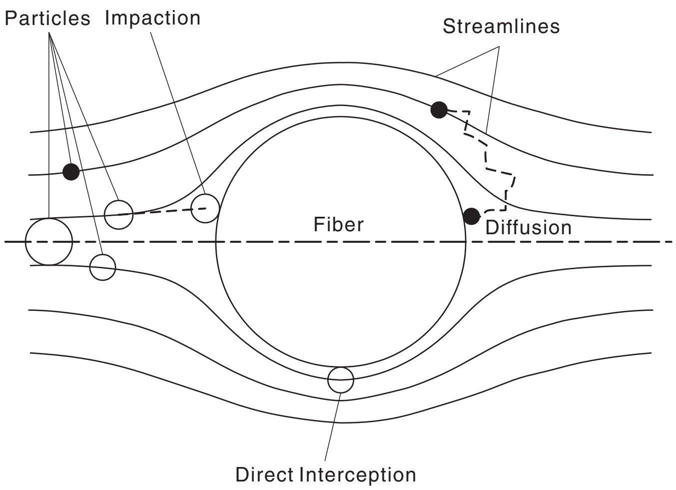

FIG. 1. The sketch of particle collected by fiber.

Downloaded by [University of Delaware] at 19:53 16 June 2012

theoretical studies of fibrous filtration. The works of Kirsch and Fuchs (1968); Yeh and Liu (1974a, 1974b), employed Kuwabara's viscous flow field through an ensemble of fibers to numerically calculate single fiber efficiencies due to diffusion, impaction, and interception.

With the advancement of technology, synthetic fiber can be made in various shapes, including ellipse, square, and rectangular cross sections to fibers with complex, multilegged cross sections (Homonoff and Dugan 2001), and the manufactured nanofibers are also available (Podgorski et al. 2006; Przekop and Gradon 2008). As noncircular fibers per unit volume can offer more surface area than circular fibers, so noncircular fibers can improve the filter performance. Some researchers have utilized analytical and numerical procedures to predict velocity fields and drag for fluid flow around fibers with square or rectangular cross sections (Brown 1984; Fardi and Liu 1992a, 1992b; Wang 1996; Ouyang and Liu 1998; Zhu et al. 2000; Cao et al. 2004). As elliptical fibers may be used in a simple model of dust loading, the studying of elliptical fibers has extra significance. Raynor (2002) obtained analytical solutions to flow and drag for elliptical fibers using the cell model, and has obtained empirical expressions for predicting the single-fiber efficiency for particle collection by the interception mechanism (Raynor 2008). Wang (Wang et al. 2008; Wang and Pui 2009) carried out numerical simulation to investigate filtration by fibers with elliptical cross sections. The simulation covers mechanisms for particles capture due to interception, inertial impaction, and diffusion. Their results shows that blunt and close to circular fibers have a higher efficiency for interception and inertial impaction, whereas long and slim fibers achieve a better efficiency for particles dominated by the diffusion effect. For very small nanoparticles, the diffusion effect is important, and long and slim elliptical fibers may improve the filter performance. Yu et al. (2008, 2009) proposed a Taylor-expansionmomentmethod to study the effect of coagulation on the evolution of nanoparticle in Brownian motion. Hosseini and Tafreshi (2010, 2011) investigated the effects of fibers' cross-sectional shape on the performance of a fibrous filter in the slip and no-slip flow regimes. Their numerical results indicated that the cross-sectional shape of nanofibers weakly affects the collection efficiency. For nanofibers, the minute dimensions can promote the aerodynamic slip, which will significantly improve the performance of an air filter. The particles in flows may be nonspherical particles, which will complicate particle dynamics because the orientation and the rotational motion are strongly coupled with the translation motion (Lin and Zhang 2002; Lin et al. 2003; Lin et al. 2004).

The viscous flow assumption is reasonable for the majority of filter applications. It was identified that the transition from viscous to potential flow occurs when the Reynolds number is about 80 (Viswanathan 1998). For particle-laden flow, the Reynolds number is usually high enough, and the applications of potential flow are possible. In the present study, starting with a solution for the velocity field around fibers with elliptical cross-sections based on Zhukovsky conversion, an exact formula for predicting the interception efficiency of a particle over an elliptic fiber collector is developed.

THEORY AND METHOD

Consider a potential flow of incompressible fluid over a two-dimensional object. The velocity potential and the stream function have some striking conjugate properties. These properties are summarized in the statement that the complex potential is an analytic function of $z(x, y)$ in the region of the z-plane occupied by the flow, meaning that the complex potential has a unique derivative with respect to z at all points in the flow. Conversely, any analytic function of z can be regarded as the complex potential of a certain flow field. Thus, simply by choosing different mathematical forms of complex potential function, we obtain possible forms of the potential functions and stream functions; although it may happen that the flow fields represented are not physically relevant. A more direct way of determining potential flow fields is provided by the method of conformal transformation of functions of a complex variable. In the present study, the deduction of interception efficiency of elliptical fiber is based on the theory of Zhukovsky conversion (Landau and Lifshitz 1959), which is defined as follows:

$$z = \frac{1}{2}\left(\zeta + \frac{b^2}{\zeta}\right) \quad [2]$$

in which b is a parameter in the transformation, and the inverse transformation is

$$\zeta = z + \sqrt{z^2 - b^2}. \quad [3]$$

Downloaded by [University of Delaware] at 19:53 16 June 2012

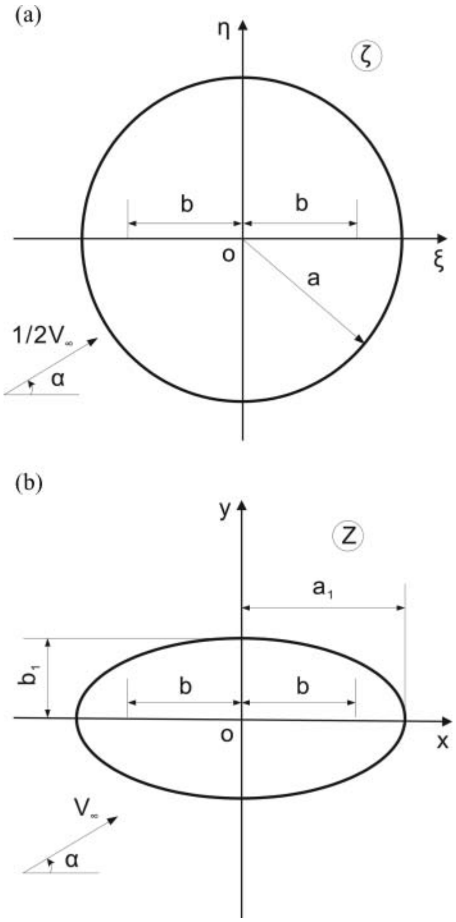

FIG. 2. Transformation from circle to ellipse.

The relationship between the coordinates in the $z(x, y)$ plane and $\zeta(\xi, \eta)$ plane is

$$x = \frac{\xi(\xi^2 + \eta^2 + 1)}{\xi^2 + \eta^2}, \quad y = \frac{\eta(\xi^2 + \eta^2 - 1)}{\xi^2 + \eta^2}. \qquad [4]$$

In order to obtain the transformation from circle to ellipse with arbitrary orientation of incoming fluid flow (α), a sketch is shown in Figure 2.

We take the procedure as follows. Firstly, the equation of a circle with radius a in the $\zeta(\xi, \eta)$ plane is

$$\xi^2 + \eta^2 = a^2. \qquad [5]$$

For convenience and without the loss of generality, we assume that $a \geq b$. The corresponding ellipse equation in $z(x, y)$ plane based on the transformation is

$$\frac{x^2}{a_1^2} + \frac{y^2}{b_1^2} = 1. \qquad [6]$$

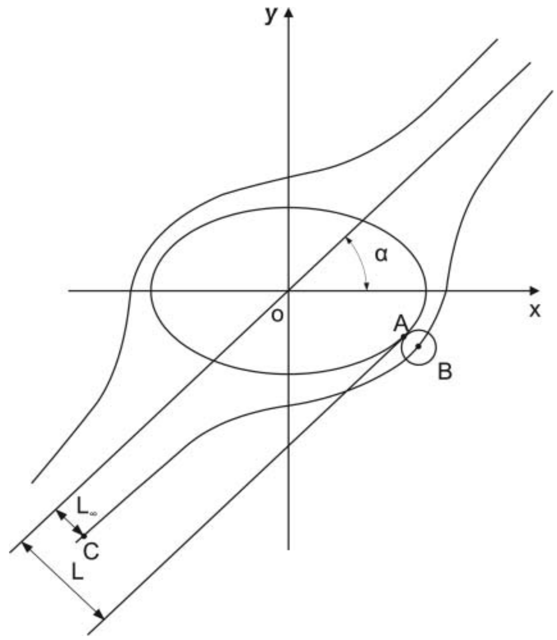

FIG. 3. The sketch of fluid pass through an ellipse.

The focus of ellipse located at $x = \pm b$, and the dimension of major and minor axis is defined as follows, respectively,

$$a_1 = \left|\frac{1}{2}\left(a + \frac{b^2}{a}\right)\right|, \quad b_1 = \left|\frac{1}{2}\left(a - \frac{b^2}{a}\right)\right|. \qquad [7]$$

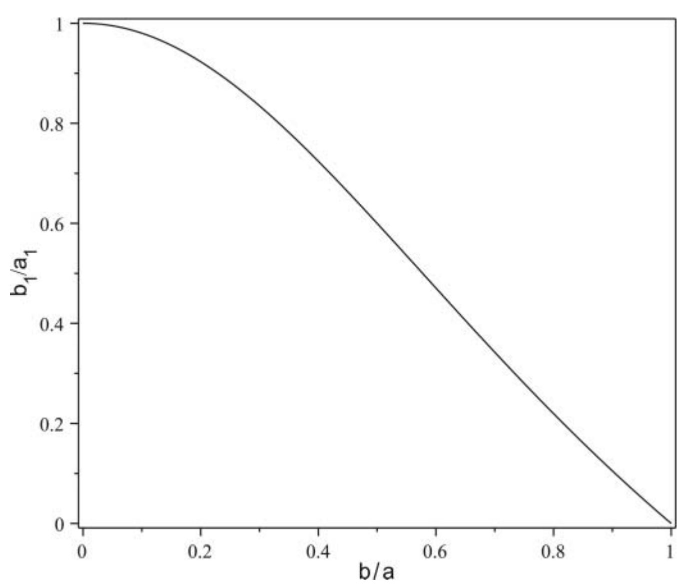

FIG. 4. The relationship between b/a and aspect ratio of ellipse b_1/a_1.

Downloaded by [University of Delaware] at 19:53 16 June 2012

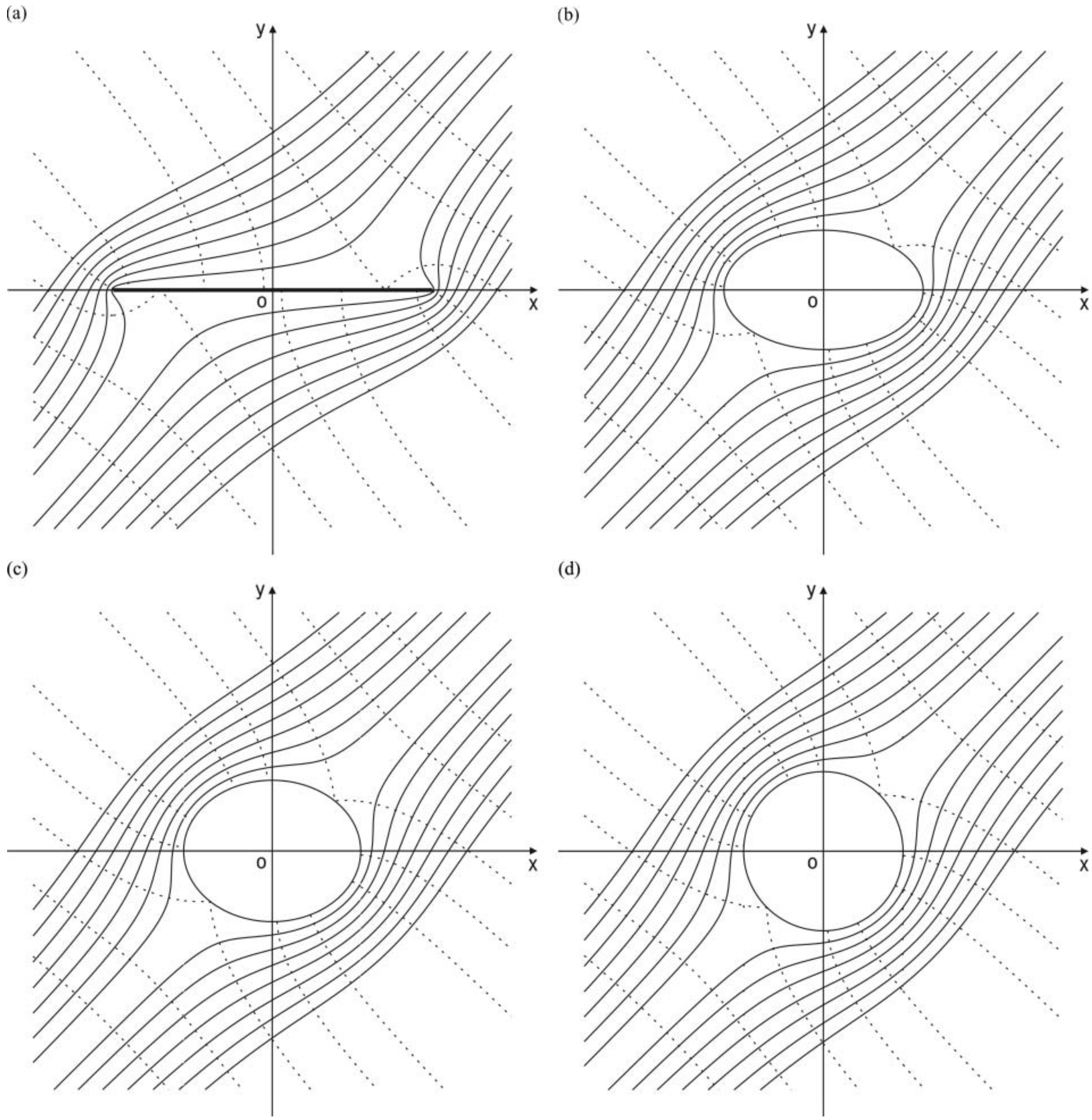

FIG. 5. The contours of stream function and potential function, (a) $b/a = 1$; (b) $b/a = 1/2$; (c) $b/a = 1/3$; (d) $b/a = 0$.

Secondly, the velocity components of incoming flow at the infinity in the $\zeta(\xi, \eta)$ plane is given by

$$\left(\frac{d\chi}{d\zeta}\right)_{\zeta=\infty} = \left(\frac{d\chi}{dz} \cdot \frac{dz}{d\zeta}\right)_{\zeta=\infty} = \frac{1}{2} v_\infty e^{-i\alpha}. \qquad [8]$$

And the complex potential function for the fluid passing through a circle can be written as,

$$\chi(\zeta) = \frac{1}{2} v_\infty \left(\zeta e^{-i\alpha} + \frac{a^2}{\zeta e^{-i\alpha}}\right). \qquad [9]$$

Then, the complex potential function in $z(x, y)$ plane can be gained using the inverse transformation Equation (3),

$$\chi(z) = \frac{1}{2} v_\infty \left[\left(z + \sqrt{z^2 - b^2}\right) \cdot e^{-i\alpha} + \frac{a^2}{\left(z + \sqrt{z^2 - b^2}\right) \cdot e^{-i\alpha}}\right]. \qquad [10]$$

Downloaded by [University of Delaware] at 19:53 16 June 2012

According to the definition of complex potential function, the potential function (real part) and stream function (imaginary part) in $z(x, y)$ plane can be written respectively as follows using the coordinate relationship Equation (3)

$$\varphi = \frac{1}{2} v_\infty (\xi \cos\alpha + \eta \sin\alpha) \left(1 + \frac{a^2}{\xi^2 + \eta^2}\right),$$
$$\psi = \frac{1}{2} v_\infty (\eta \cos\alpha - \xi \sin\alpha) \left(1 - \frac{a^2}{\xi^2 + \eta^2}\right). \quad [11]$$

Finally, the interception efficiency is the theoretical collection efficiency by a fiber for spherical particles under the assumption that both the particle inertia relative to the flow and the Brownian diffusion are negligible so that they follow air streamlines around the fiber. If the center of particle reaches 1 particle radius from the surface of a fiber, it is considered to having been collected by the fibers. The diagram is shown in Figure 3.

$$\eta_i = \frac{L_\infty}{L} \quad [12]$$

in which L_∞ is the distance between the streamline that passes through point B and the line that passes through 0 point with same direction (that means the slope of line is $\tan\alpha$) of incoming flow at infinity. L is the distance of 2 parallel lines with same slope $\tan\alpha$, and 1 line passes through zero point, the other line passes through tangent point A on the ellipse. The explicit expressions for the coordinates at point A and B, and the length for L, L_∞ are provided in the appendix.

DISCUSSION

The predicted interception efficiency depends on filter solidity, fiber geometric properties such as size and aspect ratio, the orientation of the cross section relative to the incoming flow, and particle diameter. It can be written as follows in a dimensionless form,

$$\eta_R = f\left(\frac{b}{a}, \frac{d_p}{a}, \alpha\right). \quad [13]$$

The Effect of Aspect Ratio of the Elliptic Fiber

Figure 4 shows the relationship between the aspect ratio (b_1/a_1) and the ratio of conversion parameters (b/a), it is approximately antilinear, namely, $b_1/a_1 \sim 1 - b/a$. Therefore, the effect of aspect ratio on the interception efficiency η_R can be considered in terms of b/a. Figure 5 shows the velocity field under different ratio (b/a), with the orientation angle of the incoming flow fixed at $\alpha = \pi/4$. The streamlines are divided into 2 parts that pass around different sides of the fiber. The upstream and downstream branches of this streamline are consequently given by Equation (11) for different quadrant, and the hyperbolae

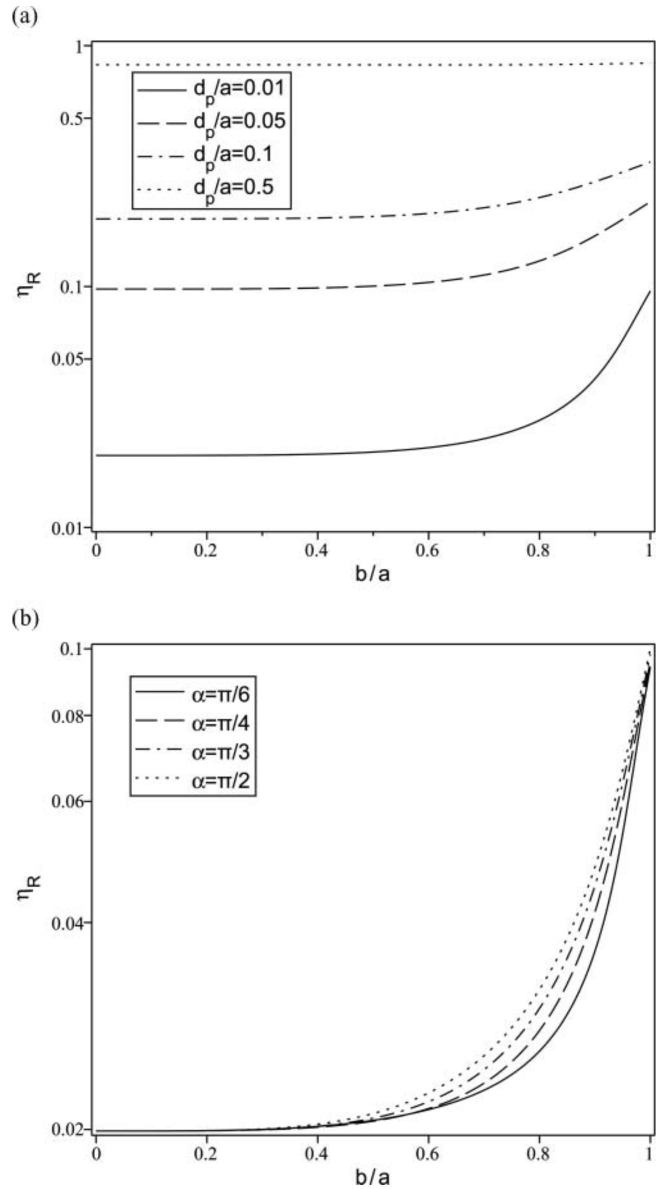

FIG. 6. The effect of ratio of aspect b/a on the interception efficiency, (a) different d_p/a at $\alpha = \pi/4$; (b) different orientation angle of incoming flow (α) at $d_p/a = 0.05$.

which are orthogonal to potential line linked with the flat plate, ellipse and circle and which asymptote to the line $y = x{\cdot}\tan\alpha$. If $b = 0$, the Equation (13) reduces to the interception efficiency of circle,

$$\eta_R = \frac{L_\infty}{L} = \left(1 + \frac{d_p}{a}\right) - \frac{1}{1 + \frac{d_p}{a}}. \quad [14]$$

It is only related to the ratio of particle size and the radius of circle, which is consistent with that of Hinds (1999). If $b = a$, the circle is transformed to the flat plate. The calculated interception efficiency in Figure 6 shows that η_R increase with

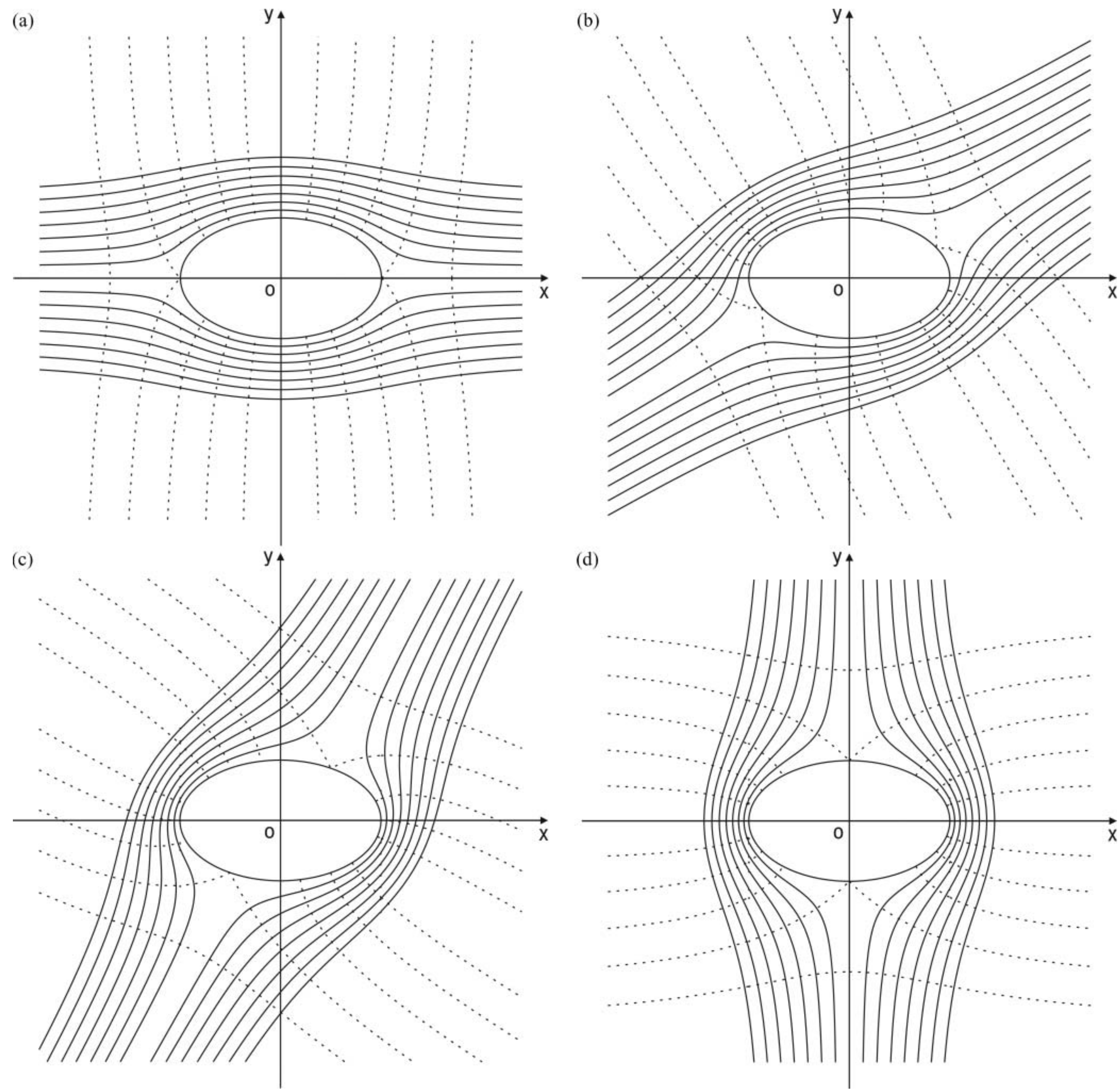

FIG. 7. The stream function and potential function for different orientation angle (α), (a) $\alpha = 0$; (b) $\alpha = \pi/6$; (c) $\alpha = \pi/3$; (d) $\alpha = \pi/2$.

Downloaded by [University of Delaware] at 19:53 16 June 2012

the ratio b/a. it confirms that noncircular fibers can significantly improve the filter performance, especially when the particle size is small.

The Effect of Orientation Angle of Incoming Flow (α)

Figure 7 shows the velocity field under 3 different orientations of the incoming flow (α). The aspect ratio of the fiber is set to 1/3, and with $\alpha = 0$, $\pi/6$, $\pi/3$, and $\pi/2$, respectively. For the 2 limiting cases ($\alpha = 0$, $\pi/2$), the streamlines are symmetric. But for any other incoming flow angle α, the streamlines are centrosymmetric; the upstream branches will be the same as the downstream branches after a half-circle rotation. Figure 8 demonstrates the relationship between the interception efficiency η_R and the orientation angle α. It can be seen from Figure 8a that the interception efficiency η_R changes slightly as the orientation angle α increases for different particle size at certain aspect ratio of ellipse ($b/a = 1/2$). In Figure 8b, there is a maximum and a minimum interception efficiency for given particle size and fiber aspect ratio. The maximum is located at $\alpha = 0$, and the corresponding α for the minimum changes for

Downloaded by [University of Delaware] at 19:53 16 June 2012

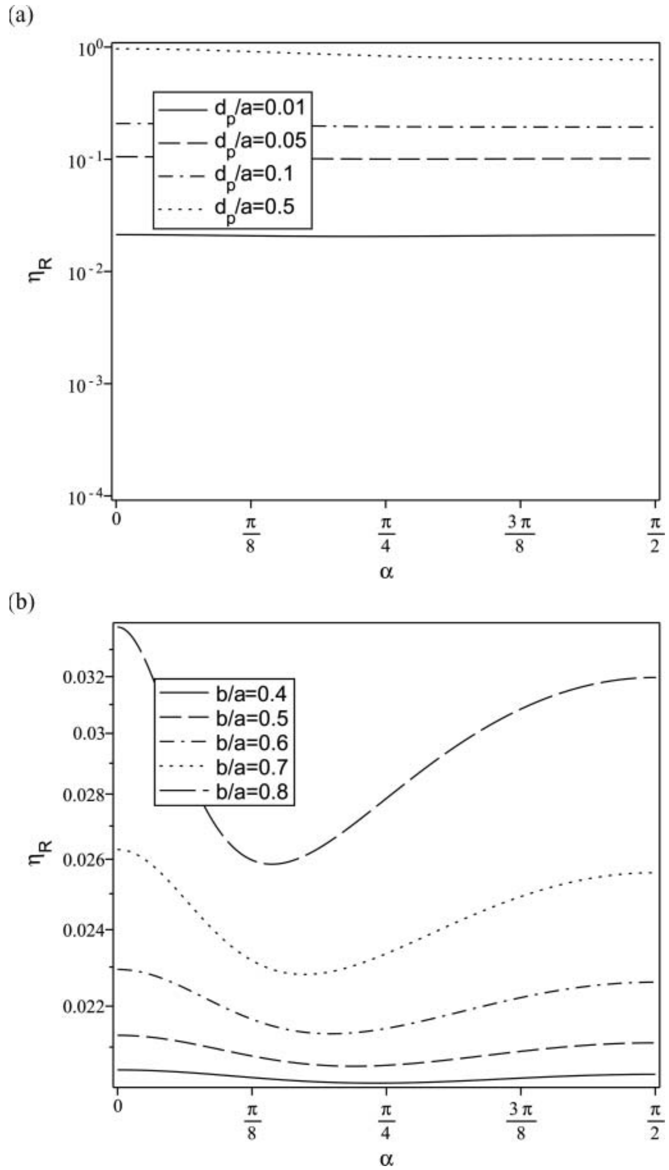

FIG. 8. The effect of orientation of incoming flow (α) on the interception efficiency, (a) different d_p/a at $b/a = 1/3$; (b) different aspect ratio b/a at $d_p/a = 0.05$.

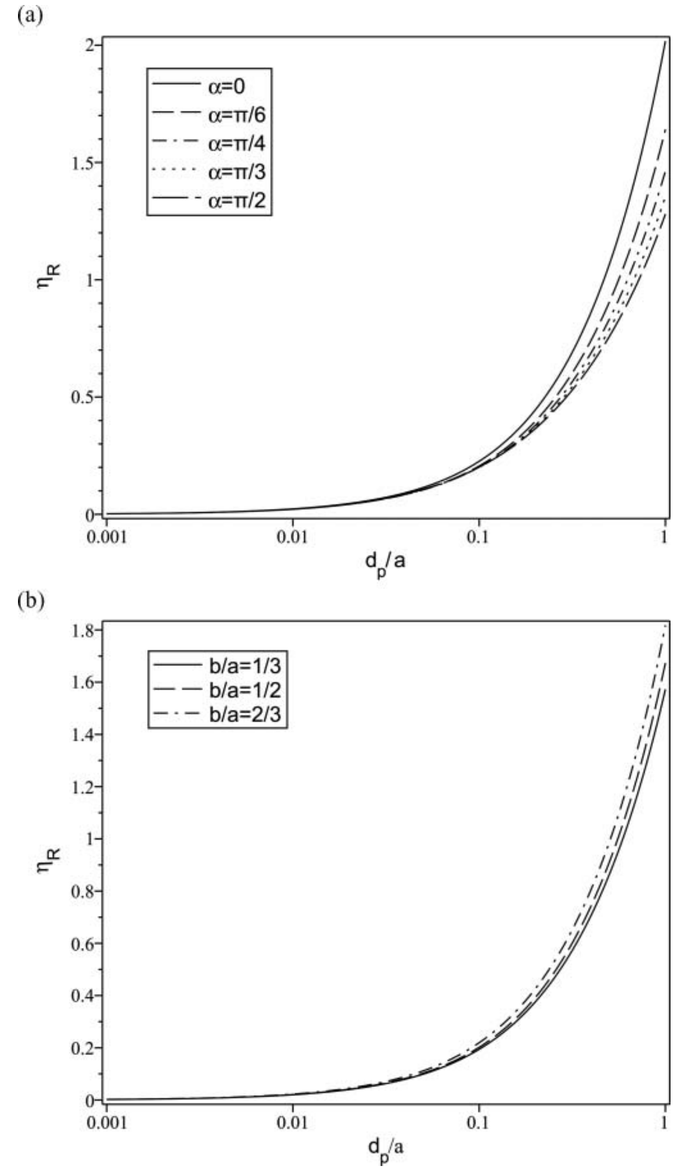

FIG. 9. The effect of particle diameter d_p/a on the interception efficiency, (a) different orientation angle of incoming flow (α) at $b/a = 1/2$; (b) different aspect ratio b/a at $\alpha = \pi/4$.

different fiber aspect ratios. And the difference between the maximum and minimum is decreased as the aspect ratio of the ellipse is increased. It trends to 0, while the ellipse becomes to circle. Clearly, the maximum interception efficiency of a noncircular fiber is much larger than that of a circle.

The Effect of Particle Size

The particle size is the crucial factor in determining the interception efficiency. Generally, for a given particle size and fiber property, the interception efficiency can be estimated approximately based on the Equation (14), it is roughly a liner relation between the interception efficiency and the ratio of particle size to circle fiber radius, the interception efficiency of a noncircular fiber has the similar trends as that of a circular fiber, which is shown in Figure 9. For small particles, the calculated interception efficiency is very low regardless what the fiber shape is. The effect of a noncircular shape becomes important mainly for larger particles.

CONCLUSION

In the present study, an exact solution for the interception efficiency of a particle onto elliptical fibers has been presented. Starting with the Zhukovsky conversion, the circle is transferred to an ellipse, and the velocity field around fibers with elliptical cross sections is solved, and then the expressions for predicting the single elliptic fiber efficiency for particle collection by the interception mechanism are developed. The result shows that the interception efficiency depends on the fiber geometric properties such as size, aspect ratio, and the orientation of the cross section relative to the incoming flow, and particle diameter. There is a maximum and a minimum interception efficiency for given particle size and fiber aspect ratio. The maximum interception efficiency occurs when the incoming flow is parallel to the major axis of an elliptical fiber, and the noncircular collector can improve the interception efficiency obviously, but it has only important impact on larger particles.

LIST OF SYMBOLS

A	the tangent point of elliptical fiber cross section
a	radius of the circular fiber cross section
a_1	length of major axis of elliptical fiber cross section
B	the center point for particles with diameter d_p just touching the ellipse
b	the parameter in the Zhukovsky conversion
b_1	length of minor axis of elliptical fiber cross section
C	the point located at streamline pass through point B at infinity
d_{p}	the diameter of small particle
K	intercept of line
L_∞	the distance between the streamline passing through point B and the line passing through 0 point with same direction ($\tan\alpha$) of fluid at infinity.
L	the distance between tangent point A of ellipse and the line through 0 point with slope $\tan\alpha$.
v_∞	the velocity of incoming flow at infinity
x	the horizontal axis coordinate of a point on elliptical plane
x_0	the horizontal axis coordinates of point B
x_1	the horizontal axis coordinates of point A
x_∞	the horizontal axis coordinate of point C
y	the vertical axis coordinate of a point on elliptical plane
y_0	the vertical axis coordinates of point B
y_1	the vertical axis coordinates of point A
y_∞	the vertical axis coordinate of point C
z	a point on elliptical plane
α	orientation angle of incoming flow
χ	the complex potential function for the fluid
ϕ	potential function
ψ	stream function
ζ	a point on circular plane
ξ	the horizontal axis coordinates of a point on circular plane
η	the vertical axis coordinates of a point on circular plane
η_R	the single fiber efficiency by interception
η_I	the single fiber efficiency by impaction
η_D	the single fiber efficiency by diffusion

REFERENCES

Brown, R. C. (1984). A Many-fibre Model of Airflow through a Fibrous Filter. *J. Aerosol Sci.*, 15:583–593.

Cao, Y. H., Cheung, C. S., and Yana, Z. D. (2004). Numerical Study of an Electret Filter Composed of an Array of Staggered Parallel Rectangular Split-type Fibers. *Aerosol Sci. Tech.*, 38:603–618.

Fardi, B., and Liu, B. Y. H. (1992a). Flow Field and Pressure Drop of Filters with Rectangular Fibers. *Aerosol Sci. Tech.*, 17:36–44.

Fardi, B., and Liu, B. Y. H. (1992b). Efficiency of Fibrous Filters with Rectangular Fibers. *Aerosol Sci. Tech.*, 17:45–58.

Happel, J. (1959). Viscous Flow Relative to Arrays of Cylinders. *AIChE J.*, 5:174–177.

Hinds, W. C. (1999). *Aerosol Technology: Properties, Behavior, and Measurement of Airborne Particles*. Wiley-Interscience, New York.

Homonoff, E., and Dugan, J. (2001). Specialty Fibers for Filtration Applications. *Advances in Filtration and Separation Technology Vol. 15*. American Filtration and Separations Society, Falls Church, VA, CD-ROM.

Hosseini, S. A., and Tafreshi, H. V. (2010). Modeling Permeability of 3-D Nanofiber Media in Slip Flow Regime. *Chem. Eng. Sci.*, 65:2249–2254.

Hosseini, S. A., and Tafreshi, H. V. (2011).'On the Importance of Fibers' Cross-sectional Shape for Air Filters Operating in the Slip Flow Regime. *Powder Technol.*, 212:425–431.

Kirsch, A. A., and Fuchs, N. A. (1967). Studies on Fibrous Aerosol Filters—II. Pressure Drops in Systems of Parallel Cylinders. *Ann. Occup. Hyg.*, 10:23–30.

Kirsch, A. A., and Fuchs, N. A. (1968). Studies on Fibrous Aerosol Filters—III. Diffusional Deposition of Aerosols in Fibrous Filters. *Ann. Occup. Hyg.*, 11:299–304.

Kuwabara, S. (1959). The Forces Experienced by Randomly Distributed Parallel Circular Cylinders or Spheres in a Viscous Flow at Small Reynolds Numbers. *J. Phys. Soc. Jpn.*, 14:522–527.

Landau, L. D., and Lifshitz, E. M. (1959). *Fluid Mechanics*. Pergamon Press, Oxford.

Lee, K. W., and Mukund, R. (2001). Filter Collection, in *Aerosol Measurement: Principles, Techniques and Applications*, P. A. Baron and K. Willeke, eds. John Wiley and Sons, New York.

Lin, J. Z., Shi, X., and Yu, Z. S. (2003). The Motion of Fibers in an Evolving Mixing Layer. *Int. J. Multiphase Flow*, 29:1355–1372.

Lin, J. Z., and Zhang, L. X. (2002). Numerical Simulation of Orientation Distribution Function of Cylindrical Particle Suspensions. *Appl. Math. Mech.*, 23:906–912.

Lin, J.Z, Zhang, W. F., and Yu, Z. S. (2004). Numerical Research on the Orientation Distribution of Fibers Immersed in Laminar and Turbulent Pipe Flows. *J. Aerosol Sci.*, 35:63–82.

Ouyang, M., and Liu, B. Y. H. (1998). Analytical Solution of Flow Field and Pressure Drop for Filters with Rectangular Fibers. *J. Aerosol Sci.*, 29:187–196.

Parker, H. W. (1977). *Air Pollution*. Prentice-Hall Inc., New Jersey, NJ.

Podgorski, A., Balazy, A., and Gradon, L. (2006). Application of Nanofibers to Improve the Filtration Efficiency of the Most Penetrating Aerosol Particles in Fibrous Filters. *Chem. Eng. Sci.*, 61:6804–6815.

Przekop, R., and Gradon, L. (2008). Deposition and Filtration of Nanoparticles in the Composites of Nano- and Microsized Fibers. *Aerosol Sci. Tech.*, 42:483–493.

Raynor, P. C. (2002). Flow Field and Drag for Elliptical Filter Fibers. *Aerosol Sci. Tech.*, 36:1118–1127.

Raynor, P. C. (2008). Single-Fiber Interception Efficiency for Elliptical Fibers. *Aerosol Sci. Tech.*, 42:357–368.

Song, X. Q., Lin, J. Z., Zhao, J. F., and Shen, T. Y. (1996). Research on Reducing Erosion by Adding Ribs on the Wall in Particulate Two-phase Flows. *Wear*, 1:1–7.

Viswanathan S. (1998). An Improved Single Droplet Collection Efficiency for the Intermediate Flow Regime. *Particul. Sci. Tec.*, 16(3):215–227.

Wang, C. Y. (1996). Stokes Flow through an Array of Rectangular Fibers. *Int. J. Multiphase Flow*, 22:185–194.

Downloaded by [University of Delaware] at 19:53 16 June 2012

Wang, J., Kim, S. C., and Pui, D. Y. H. (2008). Investigation of the Figure of Merit for Filters with a Single Nanofiber Layer on a Substrate. *J. Aerosol Sci.*, 39:323–334.
Wang, J., and Pui, D. Y. H. (2009). Filtration of Aerosol Particles by Elliptical Fibers: a Numerical Study. *J. Nanoparticle Res.*, 11:185–196.
Yeh, H., and Liu, B. Y. H. (1974a). Aerosol Filtration by Fibrous Filters-I. Theoretical. *J. Aerosol Sci.*, 5:191–204.
Yeh, H., and Liu, B. Y. H. (1974b). Aerosol Filtration by Fibrous Filters-II. Experimental. *J. Aerosol Sci.*, 5:205–217.
Yu M. Z., Lin J. Z. (2009). Taylor-expansion Moment Method for Agglomerate Coagulation due to Brownian Motion in the Entire Size Regime. *J. Aerosol Sci.*, 40(6):549–562.
Yu M. Z., Lin J. Z., and Chan T. L. (2008). A New Moment Method for Solving the Coagulation Equation for Particles in Brownian Motion. *Aerosol Sci. Tech.*, 42(9):705–713
Zhu, C., Lin, C., and Cheung, C. S. (2000). Inertial Impaction-dominated Fibrous Filtration with Rectangular or Cylindrical Fibers. *Powder Technol.*, 112:149–162.

Downloaded by [University of Delaware] at 19:53 16 June 2012

APPENDIX

The coordinates for the tangent point of ellipse A (x_1, y_1) can be calculated easily,

$$x_1 = \frac{a_1^2 \sin\alpha}{\sqrt{a_1^2 \sin^2\alpha + b_1^2 \cos^2\alpha}},$$
$$y_1 = -\frac{b_1^2 \cos\alpha}{\sqrt{a_1^2 \sin^2\alpha + b_1^2 \cos^2\alpha}}, \qquad \text{[A.1]}$$

then the point B (x_0, y_0) for particles with diameter d_p just pass by the ellipse can be expressed as

$$x_0 = x_1 + \frac{d_p}{2}\sin\alpha, \quad y_0 = y_1 - \frac{d_p}{2}\cos\alpha. \qquad \text{[A.2]}$$

The distance between the tangent point A and the line through the origin with a slope $\tan\alpha$ is

$$L = \frac{|\tan\alpha \cdot x_1 - y_1|}{\sqrt{1+\tan^2\alpha}} = \sqrt{a_1^2 \sin^2\alpha + b_1^2\cos^2\alpha}. \qquad \text{[A.3]}$$

Any point $C(x_\infty, y_\infty)$ located at streamline at the infinity will be a line with the slope $\tan\alpha$, and the line can be written as follows:

$$y_\infty = \tan\alpha \cdot x_\infty + K \qquad \text{[A.4]}$$

in which the K is the intercept. The distance between line through point $C(x_\infty, y_\infty)$ and line through the origin with the same slope α can be written as

$$L_\infty = |K\cos\alpha| = |x_\infty \sin\alpha - y_\infty\cos\alpha|, \qquad \text{[A.5]}$$

the streamline at point C is the same as that of point B, so that

$$\psi(x_\infty, y_\infty) = \psi(x_0, y_0) \qquad \text{[A.6]}$$

The streamline at the point C (x_∞, y_∞) can be simplified as

$$\begin{aligned}\psi(x_\infty, y_\infty) &= \frac{1}{2}v_\infty\left[2(-x_\infty\sin\alpha + y_\infty\cos\alpha)\right.\\ &\quad \left.+ \frac{a^2}{2(x_\infty^2+y_\infty^2)}(x_\infty\sin\alpha - y_\infty\cos\alpha)\right]\\ &= v_\infty(-x_\infty\sin\alpha + y_\infty\cos\alpha),\end{aligned} \qquad \text{[A.7]}$$

and the streamline at point $B(x_0, y_0)$ can be written as

$$\psi(x_0, y_0) = -\frac{1}{2}v_\infty(\eta\cos\alpha - \xi\sin\alpha)\left(1 - \frac{a^2}{\xi^2+\eta^2}\right), \qquad \text{[A.8]}$$

then the L_∞ is found to be,

$$L_\infty = \left|\frac{\psi(x_0, y_0)}{v_\infty}\right| = \frac{1}{2}\left|(\eta_0\cos\alpha - \xi_0\sin\alpha)\left(1-\frac{a^2}{\xi_0^2+\eta_0^2}\right)\right| \qquad \text{[A.9]}$$

in which the coordinates in the $\zeta(\xi, \eta)$ plane can be calculated based on that of the corresponding $z(x, y)$ plane in the fourth quadrant as shown in the Figure 3 as

$$\xi_0 = x_0 + \sqrt{\frac{(x_0^2 - y_0^2 - b^2) + \sqrt{(x_0^2-y_0^2-b^2)^2 + 4x_0^2y_0^2}}{2}},$$
$$\eta_0 = y_0 - \sqrt{\frac{-(x_0^2 - y_0^2 - b^2) + \sqrt{(x_0^2-y_0^2-b^2)^2 + 4x_0^2y_0^2}}{2}}, \qquad \text{[A.10]}$$

which can be obtained by solving the Equation (4), and the interception efficiency becomes

$$\eta_R = \frac{L_\infty}{L} = \frac{\left|(\eta_0\cos\alpha - \xi_0\sin\alpha)\left(1-\frac{a^2}{\xi_0^2+\eta_0^2}\right)\right|}{2\sqrt{a_1^2\sin^2\alpha + b_1^2\cos^2\alpha}}. \qquad \text{[A.11]}$$

The formula for interception efficiency is only related to the parameter (a, b) which determines the shape of ellipse, particle size (d_p) and the orientation angle (α). In order to discuss it conveniently, the interception efficiency can be considered as a function in terms of the following parameters

$$\eta_R = f\left(\frac{b}{a}, \frac{d_p}{a}, \alpha\right). \qquad \text{[A.12]}$$